

## The $\eta'g^*g^{(*)}$ Vertex Including the $\eta'$ -Meson Mass

A. Ali<sup>1</sup>

*Theory Division, CERN, CH-122 Geneva 23, Switzerland*

and

A.Ya. Parkhomenko<sup>2</sup>

*Institut für Theoretische Physik, Universität Bern,  
CH-3012 Bern, Switzerland*

### Abstract

The  $\eta'g^*g^{(*)}$  effective vertex function is calculated in the QCD hard-scattering approach, taking into account the  $\eta'$ -meson mass. We work in the approximation in which only one non-leading Gegenbauer moment for both the quark-antiquark and the gluonic light-cone distribution amplitudes for the  $\eta'$ -meson is kept. The vertex function with one off-shell gluon is shown to have the form (valid for  $|q_1^2| > m_{\eta'}^2$ )  $F_{\eta'g^*g}(q_1^2, 0, m_{\eta'}^2) = m_{\eta'}^2 H(q_1^2)/(q_1^2 - m_{\eta'}^2)$ , where  $H(q_1^2)$  is a slowly varying function, derived analytically in this paper. The resulting vertex function is in agreement with the phenomenologically inferred form of this vertex obtained from an analysis of the CLEO data on the  $\eta'$ -meson energy spectrum in the decay  $\Upsilon(1S) \rightarrow \eta'X$ . We also present an interpolating formula for the vertex function  $F_{\eta'g^*g}(q_1^2, 0, m_{\eta'}^2)$  for the space-like region of the virtuality  $q_1^2$ , which satisfies the QCD anomaly normalization for on-shell gluons and the perturbative-QCD result for the gluon virtuality  $|q_1^2| \gtrsim 2 \text{ GeV}^2$ .

---

<sup>1</sup>On leave of absence from Deutsches Elektronen-Synchrotron DESY, Hamburg.

<sup>2</sup>On leave of absence from Department of Theoretical Physics, Yaroslavl State University, Sovetskaya 14, 150000 Yaroslavl, Russia.

# 1 Introduction

We reanalyze the  $\eta'g^*g^{(*)}$  vertex involving two gluons and the  $\eta'$ -meson, in which one or both of the gluons can be virtual. The  $\eta'g^*g^{(*)}$  effective vertex function (or the  $\eta'$  – gluon transition form factor) enters in a number of decays such as  $J/\psi \rightarrow \eta'\gamma$ ,  $B \rightarrow (\pi, \rho, K, K^*)\eta'$ ,  $B \rightarrow \eta'X_s$ ,  $\Upsilon \rightarrow \eta'X$ ,  $\Upsilon \rightarrow \eta'\gamma$ , and hadronic production processes, such as  $N + N(\bar{N}) \rightarrow \eta'X$ , and hence is of great phenomenological importance. Its electromagnetic counterpart, namely the vertex  $\eta'\gamma^*\gamma$  (equivalently the  $\eta' - \gamma$  transition form factor) has been measured in the process  $\gamma\gamma^* \rightarrow \eta'$ , and analyzed in the perturbative QCD approach to exclusive processes. There is no direct experimental measurement of its QCD analogue, i.e., the process  $gg^* \rightarrow \eta'$ , but inclusive decays of the heavy mesons such as  $B \rightarrow \eta'X_s$  and  $\Upsilon(1S) \rightarrow \eta'X$  are probably as close as one could get phenomenologically to the underlying vertex.

A first attempt to describe the  $\eta'g^*g$  vertex in terms of the convolution of the distribution amplitudes (DAs) of the  $\eta'$ -meson in the lowest twist (twist-two) approximation and a hard-scattering kernel, involving the perturbatively calculable processes  $\bar{q}q \rightarrow gg$  and  $gg \rightarrow gg$ , was undertaken in Ref. [1]. In an earlier paper [2], we extended this analysis to the case involving two virtual gluons, i.e. the vertex  $\eta'g^*g^*$ , and studied the effect of including the transverse momentum of the partons in the  $\eta'$ -meson using the Sudakov formalism. Subsequent to this detailed study, the  $\eta'g^*g^*$  vertex was studied in Refs. [3] and [4], ignoring the transverse momentum effects. The latter of the two included power corrections in  $1/Q^{2n}$  by using the running coupling constant method in the standard hard-scattering approach. However, both of these papers, as well as the earlier ones, neglected the  $\eta'$ -meson mass effects. While ignoring the meson mass is an excellent approximation for the pion-photon transition form factor (equivalently the  $\pi\gamma^*\gamma$  vertex), this is not expected to be quantitatively reliable for the case of the  $\eta'$ -meson due to its large mass,  $m_{\eta'} = 958$  MeV, in particular for the lower  $Q^2$  region, where  $Q^2$  is the virtuality in the  $\eta'g^*g^{(*)}$  vertex. We present an improved calculation of the  $\eta'g^*g^*$  effective vertex function including the  $\eta'$ -meson mass. In doing this, we also correct an error in our earlier paper [2] due to an inappropriate choice of the projection operator of the  $\eta'$ -meson onto the two-gluon state.

A phenomenological form for the  $\eta' - g$  transition form factor was proposed by Kagan and Petrov some time ago [5]:

$$F_{\eta'g^*g}(q_1^2, 0, m_{\eta'}^2) = \frac{m_{\eta'}^2 H(q_1^2, 0, m_{\eta'}^2)}{q_1^2 - m_{\eta'}^2}. \quad (1)$$

As an explicit form for the function  $H(q_1^2, 0, m_{\eta'}^2)$ , these authors suggested to neglect the  $q_1^2$ -dependence and approximate this function as a constant, with  $H(q_1^2, 0, m_{\eta'}^2) \simeq 1.8 \text{ GeV}^{-1}$  extracted from the data on the decay  $J/\psi \rightarrow \eta'\gamma$  [6]. This phenomenological transition form factor is in qualitative agreement with the  $\eta'$ -meson energy spectrum near the upper end of the spectrum in the process  $\Upsilon(1S) \rightarrow \eta'X$  [7], measured recently by the CLEO collaboration [8], and also analyzed by us in a recent paper [9]. We show in this paper that the form (1) of the  $\eta' - g$  transition form factor is obtained in the perturbative hard-scattering approach, if a light-cone wave-function for the  $\eta'$ -meson is used including the  $\eta'$ -meson mass.

The validity of the perturbative QCD formalism is expected to hold only above a certain gluon virtuality, which for the time-like region of  $q_1^2$  must be definitely larger than  $m_{\eta'}^2$  to avoid the pole. For the space-like region, there is no a pole for any value of  $q_1^2$  and also the effects of including the transverse momentum of the partons in the  $\eta'$ -meson wave-function are numerically not important, as shown in Ref. [2]. However, also for this case, for low values of the gluon virtuality important non-perturbative effects are present and the perturbative QCD formalism for the  $\eta'g^*g$  vertex is no longer applicable. In our numerical calculations, we shall set  $Q_0^2 = \mu_0^2 = 2 \text{ GeV}^2$ , where  $Q_0$  and  $\mu_0$  are the threshold in the evaluation of the perturbative QCD kernel and the starting point of the evolution of the  $\eta'$ -meson distribution amplitudes, respectively. For on-shell gluons, the  $\eta'g^*g$  vertex function  $F_{\eta'gg}(0, 0, m_{\eta'}^2)$  is determined by the QCD anomaly which is a non-perturbative result. We propose an interpolating formula for the vertex function  $F_{\eta'g^*g}(q_1^2, 0, m_{\eta'}^2)$ , which interpolates between the normalization of this function for on-shell gluons, as determined from the QCD anomaly, and the perturbative QCD hard-scattering result for space-like gluon virtualities with  $Q^2 \geq Q_0^2$  where  $Q^2 = |q_1^2| + m_{\eta'}^2$ . For the time-like virtuality, an interpolating formula for the vertex function remains to be worked out, as one must include the transverse-momentum effects, which are large at low values of  $q_1^2$ , in addition to the non-perturbative and the  $\eta'$ -meson mass effects.

This paper is organized as follows: In section 2, we present the  $\eta'$ -meson projection operators onto the quark-antiquark and the gluonic states, taking into account the  $\eta'$ -meson mass effects, and the leading-twist distribution amplitudes for the  $\eta'$ -meson. In section 3, we derive the  $\eta'g^*g^*$  effective vertex function in the perturbative QCD approach and discuss the region of its applicability. Numerical analysis of the effective vertex function is presented in section 4, where we have used the constraints on the Gegenbauer coefficients obtained by us [9] from the analysis of the data on the  $\Upsilon(1S) \rightarrow \eta'X$  decay, combined with the corresponding constraints from the data on the process  $\gamma\gamma^* \rightarrow \eta'$  presented in Ref. [3]. In section 5, we give an interpolating formula for the  $\eta'g^*g$  vertex function for the space-like region of the gluon virtuality. We conclude with a short summary in section 6.

## 2 The $\eta'$ -Meson Projection Operators

### 2.1 Projection onto the Quark-Antiquark State

The  $\eta'$ -meson contains both quark-antiquark and gluonic components. Being a pseudoscalar meson, its quark content can be described by the matrix element of the bilocal axial-vector operator in the  $SU(3)$  flavour-singlet state:

$$\mathcal{O}_{5\mu}^{(q)}(x, y) = \frac{1}{\sqrt{N_f}} \bar{\Psi}(x) \gamma_\mu \gamma_5 [x, y] \Psi(y), \quad (2)$$

where  $\Psi(x) = (u(x), d(x), s(x))$  is the triplet of the light quark fields in the flavour space and  $N_f = 3$ . The summation over the Dirac, colour and flavour indices is implicitly assumed in this bilocal operator. The path-ordered gauge factor,

$$[x, y] = \mathcal{P} \exp \left\{ i g_s \int_y^x dz^\mu A_\mu^B(z) t_B \right\}, \quad (3)$$

is introduced to ensure gauge invariance of the bilocal axial-vector quark operator (2). In the gauge factor (3),  $g_s$  is the QCD coupling constant,  $A_\mu^B(z)$  ( $B = 1, \dots, N_c^2 - 1$ ) is a four-potential of the gluonic field,  $t_B$  are the generators of the colour  $SU(N_c)$  group with  $N_c = 3$  being the number of the quark colours in QCD, and the integration is performed over the straight line connecting the points  $y$  and  $x$ .

Taking into account the leading-twist (twist-two), twist-three and twist-four contributions, the matrix element of the operator (2) between the vacuum and the  $\eta'$ -meson states can be presented in the form:

$$\langle 0 | \mathcal{O}_{5\mu}^{(q)}(x, -x) | \eta'(p) \rangle = i f_{\eta'} \int_0^1 du e^{i\xi(px)} \left\{ p_\mu \left[ \phi_{\eta'}^{(q)}(u) + \frac{m_{\eta'}^2}{4} x^2 \mathbb{A}(u) \right] + \frac{m_{\eta'}^2 x_\mu}{2(px)} \mathbb{B}(u) \right\}, \quad (4)$$

where  $p_\mu$  is the four-momentum of the  $\eta'$ -meson ( $p^2 = m_{\eta'}^2$ ),  $u$  and  $1-u$  are the momentum fractions carried by the quark and the antiquark inside the  $\eta'$ -meson, and  $\xi = 2u - 1$ . The function  $\phi_{\eta'}^{(q)}(u)$  is the twist-two distribution amplitude (DA), and  $\mathbb{A}(u)$  and  $\mathbb{B}(u)$  contain contributions from operators of twist-two, twist-three and twist-four. This set of the quark-antiquark two-particle DAs is completely analogous to the one defined in Ref. [10] for the case of the  $SU(3)$  flavour-octet pseudoscalar mesons. The decay constant  $f_{\eta'}$  is defined in the local limit of the matrix element (4) as

$$\langle 0 | \mathcal{O}_{5\mu}^{(q)}(0, 0) | \eta'(p) \rangle = \langle 0 | \frac{1}{\sqrt{N_f}} \bar{\Psi}(0) \gamma_\mu \gamma_5 \Psi(0) | \eta'(p) \rangle = i f_{\eta'} p_\mu. \quad (5)$$

Thus, the DAs satisfy the following normalization conditions:

$$\int_0^1 du \phi_{\eta'}^{(q)}(u) = 1, \quad \int_0^1 du \mathbb{B}(u) = 0. \quad (6)$$

The normalization condition for  $\mathbb{A}(u)$  is not fixed by Eq. (5). This DA is related to the two- and three-particle DAs of lower twists with the help of the equations of motion (see Eqs. (3.2) and (6.11) of Ref. [10]) and, thus, its form (and also the normalization) is implicitly fixed.

We now proceed to work out the DAs of the  $\eta'$ -meson on the light-cone. To that end, we construct two light-like vectors  $z_\mu$  and  $P_\mu$  ( $z^2 = 0$  and  $P^2 = 0$ ) of the same dimensions as the two vectors  $x_\mu$  and  $p_\mu$  at hand:

$$z_\mu = x_\mu - \frac{p_\mu}{m_{\eta'}^2} \left[ (px) - \sqrt{(px)^2 - m_{\eta'}^2 x^2} \right], \quad (7)$$

$$P_\mu = p_\mu - \frac{m_{\eta'}^2 x_\mu}{(px) + \sqrt{(px)^2 - m_{\eta'}^2 x^2}}. \quad (8)$$

Their scalar product has a rather complicated form:

$$(Pz) = \frac{2 \left[ (px)^2 - m_{\eta'}^2 x^2 \right]}{(px) + \sqrt{(px)^2 - m_{\eta'}^2 x^2}}, \quad (9)$$

which, however, can be simplified if one assumes that the separation between the quark and the antiquark inside the  $\eta'$ -meson is light-like ( $x_\mu = z_\mu$  and  $x^2 = z^2 = 0$ ). The light-like momentum  $P_\mu$  introduced in Eq. (8) then takes a simple form:

$$P_\mu = p_\mu - \frac{m_{\eta'}^2 z_\mu}{2(pz)}, \quad (Pz) = (pz) = (px). \quad (10)$$

In terms of such light-like vectors, one can give definitions of the DAs of the  $\eta'$ -meson on the light-cone (similar to the ones for the  $\pi$ -meson [10]) following from the matrix element of the axial-vector current:

$$\langle 0 | \mathcal{O}_{5\mu}^{(q)}(z, -z) | \eta'(p) \rangle = i f_{\eta'} \int_0^1 du e^{i\xi(pz)} \left[ P_\mu \phi_{\eta'}^{(q)}(u) + \frac{m_{\eta'}^2 z_\mu}{2(Pz)} g_{\eta'}^{(q)}(u) \right]. \quad (11)$$

Comparing it with Eq. (4), one obtains the relation:

$$\mathbb{B}(u) = g_{\eta'}^{(q)}(u) - \phi_{\eta'}^{(q)}(u), \quad (12)$$

implying that the Lorentz invariant amplitudes  $\phi_{\eta'}^{(q)}(u)$  and  $\mathbb{B}(u)$  can be interpreted as the  $\eta'$ -meson DAs of the nonlocal axial-vector operator at a strictly light-like separation. It is easy to see the usual normalization conditions of the light-cone DAs:

$$\int_0^1 du \phi_{\eta'}^{(q)}(u) = 1, \quad \int_0^1 du g_{\eta'}^{(q)}(u) = 1. \quad (13)$$

Two more bilocal matrix elements define DAs of the twist-three:

$$\langle 0 | \frac{1}{\sqrt{N_f}} \bar{\Psi}(x) \gamma_5 [x, -x] \Psi(-x) | \eta'(p) \rangle = -i f_{\eta'} \mu_{\eta'} \int_0^1 du e^{i\xi(px)} \phi_p^{(\eta')}(u), \quad (14)$$

$$\begin{aligned} \langle 0 | \frac{1}{\sqrt{N_f}} \bar{\Psi}(x) \sigma_{\alpha\beta} \gamma_5 [x, -x] \Psi(-x) | \eta'(p) \rangle &= -\frac{i}{3} f_{\eta'} \mu_{\eta'} \left[ 1 - \frac{m_{\eta'}^2}{\mu_{\eta'}^2} \right] \\ &\times (p_\alpha x_\beta - p_\beta x_\alpha) \int_0^1 du e^{i\xi(px)} \phi_\sigma^{(\eta')}(u), \end{aligned} \quad (15)$$

where  $\mu_{\eta'} = m_{\eta'}^2 / (2m_u + 2m_d + 2m_s)$  is a chirally enhanced factor including the masses  $m_q$  ( $q = u, d, s$ ) of the light quarks. Note that after the transition to the light-cone vectors  $P_\mu$  and  $z_\mu$ , the forms of Eqs. (14) and (15) are not changed in the twist-three approximation and, thus, the Lorentz invariant twist-three DAs coincide with the light-cone twist-three DAs. There also exist twist-three DAs defined by the matrix elements of the three-particle (quark-antiquark-gluon) operators. For the light pseudoscalar flavour-octet mesons, it has been shown in Ref. [10] that their contributions are numerically small. We expect that this also holds for the SU(3) flavour-singlet meson and neglect such contributions. In

general, one should also take into account the twist-four DAs from the matrix elements of three-particle nonlocal operators. The self-consistent set of such DAs was introduced in Ref. [11, 12] for light pseudoscalar flavour-octet mesons; their explicit updated forms can be found in Ref. [10]. While the effect of the chirally enhanced bilocal matrix elements of higher twist operators is an interesting issue to study, we neglect here the twist-three and twist-four contributions to the  $\eta'$ -meson light-cone wave-function.

Starting from Eq. (11), one can calculate the light-cone projection operator of the  $\eta'$ -meson onto the quark-antiquark state in the leading-twist (twist-two) approximation<sup>3</sup>:

$$\langle 0 | \bar{\Psi}_{i\alpha a}(z) \Psi_{j\beta b}(-z) | \eta'(p) \rangle = \frac{if_{\eta'}}{4N_c} [\gamma_5(P\gamma)]_{ji} \delta_{\beta\alpha} \frac{\delta_{ba}}{\sqrt{N_f}} \int_0^1 du e^{i\xi(pz)} \phi_{\eta'}^{(q)}(u), \quad (16)$$

where the two sets of indices  $(i\alpha a)$  and  $(j\beta b)$  describe the components of the quark  $\bar{\Psi}(z)$  and antiquark  $\Psi(-z)$  fields in the Dirac, colour and flavour spaces, respectively, and  $(P\gamma) = P^\mu \gamma_\mu$ . After the Fourier transformation of Eq. (16) to the momentum space (see Eqs. (A.4) and (A.5) in Ref. [3]), the result can be presented in the form:

$$\frac{if_{\eta'}}{4N_c} [\gamma_5(P\gamma)]_{ji} \delta_{\beta\alpha} \frac{\delta_{ba}}{\sqrt{N_f}} \phi_{\eta'}^{(q)}(u) = 2(np) \int \frac{dz^-}{2\pi} e^{-i\xi(pz)} \langle 0 | \bar{\Psi}_{i\alpha a}(z) \Psi_{j\beta b}(-z) | \eta'(p) \rangle, \quad (17)$$

where  $z_\mu = z^- n_\mu$ , and  $n_\mu$  is a dimensionless light-like vector ( $n^2 = 0$ ). In the momentum space, the quantity

$$\mathcal{P}_{j\beta b; i\alpha a}^{(q)} = \frac{1}{4N_c} [\gamma_5(P\gamma)]_{ji} \delta_{\beta\alpha} \frac{\delta_{ba}}{\sqrt{N_f}} \quad (18)$$

can be interpreted as the  $\eta'$ -meson light-cone projection operator onto the state of the incoming quark and antiquark [13]. The quark-antiquark twist-two light-cone DA,  $\phi_{\eta'}^{(q)}(u)$ , can be defined as follows:

$$if_{\eta'} \phi_{\eta'}^{(q)}(u) = 2 \int \frac{dz^-}{2\pi} e^{-i\xi(Pz)} \langle 0 | n^\mu \mathcal{O}_{5\mu}^{(q)}(z, -z) | \eta'(p) \rangle, \quad (19)$$

where the bilocal axial-vector operator is defined in Eq. (2). Some words about the vector  $n_\mu$  are in order. While well-defined in the position space through the light-like separation between the constituents inside the  $\eta'$ -meson, this vector is arbitrary in the momentum space and its explicit choice is dictated by the process at hand. The most natural choice of this vector is the four-momentum of some massless particle which appears in a given process (see, for example, Ref. [3, 14]). If such a vector is absent, the light-like vector  $n_\mu$  should be constructed from existing four-vectors explicitly. A representation of the vector  $n_\mu$  will be given in the next section.

---

<sup>3</sup>The path-ordered gauge factor (3) is assumed to be between the quark fields and is suppressed to simplify the presentation.

## 2.2 Projection onto the Gluonic State

The gluonic content of the  $\eta'$ -meson can be described with the help of the partially traceless and symmetric bilocal gluonic operator<sup>4</sup>:

$$\tilde{\mathcal{O}}_{\mu\nu}^{(g)}(x, y) = \frac{1}{2} \left[ G_{\mu\alpha}(x)[x, y] \tilde{G}_\nu^\alpha(y) + G_{\nu\alpha}(x)[x, y] \tilde{G}_\mu^\alpha(y) \right] - \frac{g_{\mu\nu}}{4} G_{\alpha\beta}(x)[x, y] \tilde{G}^{\alpha\beta}(y), \quad (20)$$

where  $G_{\mu\nu}^A(x)$  and  $\tilde{G}_{\mu\nu}^A(x)$  are the gluonic field strength tensor and its dual tensor, respectively, and the path-ordered gauge factor  $[x, y]$  should be taken here in the adjoint representation of the colour  $SU(N_c)$  group. In the above operator, the summation over the colour indices is implicitly assumed. Starting from the gluonic operator (20), one can introduce the gluonic twist-two, twist-three, and twist-four DAs, similar to the quark-antiquark DAs (4) corresponding to the axial-vector bilocal operator (2), as follows:

$$\begin{aligned} \langle 0 | \tilde{\mathcal{O}}_{\mu\nu}^{(g)}(x, -x) | \eta'(p) \rangle &= \frac{f_{\eta'} C_F}{2\sqrt{N_f}} \int_0^1 du e^{i\xi(px)} \left\{ \left[ p_\mu p_\nu - \frac{m_{\eta'}^2}{4} g_{\mu\nu} \right] \left[ \phi_{\eta'}^{(g)}(u) + m_{\eta'}^2 x^2 \mathbb{C}(u) \right] \right. \\ &\quad \left. + \left[ 2 \frac{p_\mu x_\nu + p_\nu x_\mu}{(px)} - g_{\mu\nu} \right] \frac{m_{\eta'}^2}{4} \mathbb{D}(u) \right\}, \end{aligned} \quad (21)$$

where  $C_F = (N_c^2 - 1)/(2N_c)$ .

In the local limit, the bilocal gluonic operator (20) vanishes [ $\tilde{\mathcal{O}}_{\mu\nu}^{(g)}(0, 0) = 0$ ] due to the following operator relation:

$$G_{\mu\alpha}(0) \tilde{G}_\nu^\alpha(0) = \frac{g_{\mu\nu}}{4} G_{\alpha\beta}(0) \tilde{G}^{\alpha\beta}(0), \quad (22)$$

which gives the normalization conditions for the Lorentz-invariant gluonic DAs introduced in Eq. (21):

$$\int_0^1 du \phi_{\eta'}^{(g)}(u) = 0, \quad \int_0^1 du \mathbb{D}(u) = 0. \quad (23)$$

These conditions leave an arbitrariness in the choice of a constant prefactor in the matrix element (21). The motivation of the choice made in this paper will be commented in the next subsection. The normalization of the DA  $\mathbb{C}(u)$  is not determined in the local limit of the operator (20), but this DA can be related with the other two- and three-particle DAs of lower twists using the equations of motion in the same manner as has been done for the flavour-octet pseudoscalar mesons [10, 11, 12].

Following the discussion in the preceding subsection, let us assume that the two gluons are separated by the light-like vector  $x_\mu = z_\mu$  ( $x^2 = z^2 = 0$ ). Thus, the matrix element of the bilocal gluonic operator can be presented in terms of the gluonic light-cone DAs:

$$\langle 0 | \tilde{\mathcal{O}}_{\mu\nu}^{(g)}(z, -z) | \eta'(p) \rangle = \frac{f_{\eta'} C_F}{2\sqrt{N_f}} \int_0^1 du e^{i\xi(pz)} \left\{ P_\mu P_\nu \phi_{\eta'}^{(g)}(u) \right. \quad (24)$$

---

<sup>4</sup>The method of construction of the completely traceless quark-antiquark and gluonic operators can be found in Refs. [15] and [16].

$$+ \left[ 2 \frac{P_\mu z_\nu + P_\nu z_\mu}{(Pz)} - g_{\mu\nu} \right] \frac{m_{\eta'}^2}{4} g_{\eta'}^{(g)}(u) \Big\},$$

where the four-vector  $P_\mu$  is defined in Eq. (10). Comparison of this equation with Eq. (21) leads to the following relation:

$$\mathbb{D}(u) = g_{\eta'}^{(g)}(u) - \phi_{\eta'}^{(g)}(u). \quad (25)$$

This shows that the Lorentz-invariant DAs,  $\phi_{\eta'}^{(g)}(u)$  and  $\mathbb{D}(u)$ , are connected with the light-cone DAs of the  $\eta'$ -meson defined by the bilocal operator (20) with a strictly light-like separation between the gluon fields, in the same manner as for the quark-antiquark DAs,  $\phi_{\eta'}^{(q)}(u)$  and  $\mathbb{B}(u)$ , defined by the bilocal axial-vector operator (2). The normalization conditions for the gluonic light-cone DAs are:

$$\int_0^1 du \phi_{\eta'}^{(g)}(u) = 0, \quad \int_0^1 du g_{\eta'}^{(g)}(u) = 0. \quad (26)$$

As we restricted ourselves to the leading-twist part of the quark-antiquark component of the  $\eta'$ -meson only, we also do not consider any further the higher-twist DAs in the gluonic component of the  $\eta'$ -meson.

The gauge-invariant definition of the gluonic light-cone DAs (24) is given in terms of the gluonic field strength tensor  $G_{\mu\nu}^A(z)$  and its dual  $\tilde{G}_{\mu\nu}^A(-z)$ , though the usual Feynman rules involve the gluonic four-potential  $A_\mu^A(z)$ . A possible way to get the required matrix element is to use the relation between the field strength tensor and the four-potential in the light-cone gauge ( $n^\mu A_\mu^A(x; n) = 0$ ) [17]:

$$A_\mu^A(x; n) = n^\nu \int_0^\infty G_{\mu\nu}^A(x + \sigma n) d\sigma, \quad (27)$$

so that it can be applied to Eq. (24) after its contraction with the light-like vectors  $n^\mu$  and  $n^\nu$ . In the leading-twist approximation, the projection operator of the  $\eta'$ -meson onto the gluonic state in terms of the gluonic four-potentials can be written as follows [3]<sup>5</sup>:

$$\langle 0 | A_{[\mu}^A(z) A_{\nu]}^B(-z) | \eta'(p) \rangle = \frac{f_{\eta'} C_F}{4\sqrt{N_f}} \frac{\delta_{AB}}{2N_c C_F} \frac{\varepsilon_{\mu\nu\rho\sigma} z^\rho P^\sigma}{(zP)} \int_0^1 du e^{i\xi(pz)} \frac{\phi_{\eta'}^{(g)}(u)}{u(1-u)}, \quad (28)$$

where  $A_{[\mu}^A(x) A_{\nu]}^B(y) \equiv [A_\mu^A(x) A_\nu^B(y) - A_\nu^A(x) A_\mu^B(y)]/2$  is the bilocal operator antisymmetrized in the Lorentz indices. The gluonic matrix element (28) contains the Lorentz structure  $\varepsilon_{\mu\nu\rho\sigma} z^\rho P^\sigma / (zP)$ . To perform the Fourier transform to the momentum space, it is convenient to introduce the dimensionless light-like vector  $n_\alpha$  (its explicit form in a specific frame is given in Eq. (A.3) of Ref. [3]) so that  $z_\alpha = z^- n_\alpha$ . The light-like vector  $P_\mu$  defined by Eq. (10) becomes independent of the variable  $z^-$ :

$$P_\mu = p_\mu - \frac{m_{\eta'}^2 n_\mu}{2(pn)}, \quad (Pn) = (pn), \quad (29)$$

<sup>5</sup>Starting from here we suppress the path-ordered gauge factor  $[z, -z]$  in the matrix elements.



and the Lorentz structure under consideration transforms as

$$\varepsilon_{\mu\nu\rho\sigma} \frac{z^\rho P^\sigma}{(zP)} \longrightarrow \varepsilon_{\mu\nu\rho\sigma} \frac{n^\rho P^\sigma}{(nP)} = \varepsilon_{\mu\nu\rho\sigma} \frac{n^\rho p^\sigma}{(np)}. \quad (30)$$

Note the invariance of this Lorentz structure under the transformations  $P_\mu \rightarrow P'_\mu = P_\mu + C n_\mu$  or  $n_\mu \rightarrow n'_\mu = n_\mu + \tilde{C} P_\mu$ , where  $C$  and  $\tilde{C}$  are arbitrary factors. The last expression in Eq. (30) corresponds to the specific choice of the first factor:  $C = m_{\eta'}^2/2(np)$ . The invariance of the Lorentz structure (30) under the transformation of the light-like vector  $n_\mu$  was pointed out in Ref. [3] for the case of the massless  $\eta'$ -meson (i.e., with  $p^2 = 0$  and  $P_\mu = p_\mu$ ).

After performing the Fourier transformation of Eq. (28), we obtain the following result:

$$\frac{f_{\eta'} \delta_{AB}}{8N_c \sqrt{N_f}} \frac{\varepsilon_{\mu\nu\rho\sigma} n^\rho p^\sigma}{(np)} \frac{\phi_{\eta'}^{(g)}(u)}{u(1-u)} = 2(np) \int \frac{dz^-}{2\pi} e^{-i\xi(pz)} \langle 0 | A_{[\mu}^A(z) A_{\nu]}^B(-z) | \eta'(p) \rangle. \quad (31)$$

In the momentum space, the quantity

$$\mathcal{P}_{\mu A; \nu B}^{(g)} = \frac{i \delta_{AB}}{4N_c \sqrt{N_f}} \frac{\varepsilon_{\mu\nu\rho\sigma} n^\rho p^\sigma}{(np)} \quad (32)$$

is the projection operator of the  $\eta'$ -meson onto the state of two incoming gluons [13]. The gluonic twist-two light-cone DA can be defined through the following matrix element:

$$f_{\eta'} \phi_{\eta'}^{(g)}(u) = \frac{4\sqrt{N_f}}{C_F(np)} \int \frac{dz^-}{2\pi} e^{-i\xi(pz)} \langle 0 | n^\mu G_{\mu\alpha}(z) n_\nu \tilde{G}^{\nu\alpha}(-z) | \eta'(p) \rangle, \quad (33)$$

where the summation over the colour indices is implicitly assumed on the right-hand side.

## 2.3 The $\eta'$ -Meson Light-Cone Distribution Amplitudes

The leading-twist light-cone DAs of the  $\eta'$ -meson can be presented as infinite series in the Gegenbauer polynomials  $C_n^{3/2}(u - \bar{u})$  for the quark-antiquark component and  $C_{n-1}^{5/2}(u - \bar{u})$  for the gluonic one [18, 19, 20, 21, 13, 22]:

$$\phi_{\eta'}^{(q)}(u, Q^2) = 6u\bar{u} \left[ 1 + \sum_{\text{even } n \geq 2} A_n(Q^2) C_n^{3/2}(u - \bar{u}) \right], \quad (34)$$

$$\phi_{\eta'}^{(g)}(u, Q^2) = u^2 \bar{u}^2 \sum_{\text{even } n \geq 2} B_n(Q^2) C_{n-1}^{5/2}(u - \bar{u}), \quad (35)$$

where  $\bar{u} = 1 - u$ , and the following notations are introduced for the Gegenbauer moments:

$$A_n(Q^2) = B_n^{(q)}(\mu_0^2) \left[ \frac{\alpha_s(\mu_0^2)}{\alpha_s(Q^2)} \right]^{\gamma_+^n} + \rho_n^{(g)} B_n^{(g)}(\mu_0^2) \left[ \frac{\alpha_s(\mu_0^2)}{\alpha_s(Q^2)} \right]^{\gamma_-^n}, \quad (36)$$

$$B_n(Q^2) = \rho_n^{(q)} B_n^{(q)}(\mu_0^2) \left[ \frac{\alpha_s(\mu_0^2)}{\alpha_s(Q^2)} \right]^{\gamma_+^n} + B_n^{(g)}(\mu_0^2) \left[ \frac{\alpha_s(\mu_0^2)}{\alpha_s(Q^2)} \right]^{\gamma_-^n}. \quad (37)$$

These equations contain the quantities  $\gamma_{\pm}^n$ , defined as:

$$\gamma_{\pm}^n \equiv \frac{1}{2} \left[ \gamma_{QQ}^n + \gamma_{GG}^n \pm \sqrt{(\gamma_{QQ}^n - \gamma_{GG}^n)^2 + 4\gamma_{QG}^n \gamma_{GQ}^n} \right], \quad (38)$$

where the anomalous dimensions  $\gamma_{ij}^n$  ( $i, j = Q, G$ ) are

$$\begin{aligned} \gamma_{QQ}^n &= \frac{C_F}{\beta_0} \left[ 3 + \frac{2}{(n+1)(n+2)} - 4 \sum_{j=1}^{n+1} \frac{1}{j} \right], \\ \gamma_{QG}^n &= \frac{C_F}{\beta_0} \frac{n(n+3)}{3(n+1)(n+2)}, \\ \gamma_{GQ}^n &= \frac{N_f}{\beta_0} \frac{12}{(n+1)(n+2)}, \\ \gamma_{GG}^n &= \frac{N_c}{\beta_0} \left[ \frac{8}{(n+1)(n+2)} - 4 \sum_{j=1}^{n+1} \frac{1}{j} \right] + 1. \end{aligned} \quad (39)$$

Here,  $\beta_0 = (11N_c - 2n_f)/3$  is the first coefficient in the expansion of the QCD  $\beta$ -function and  $n_f$  is the number of quarks with masses less than the energy scale  $Q$  entering in the DAs (34) and (35). Note the difference between the quark numbers  $N_f = 3$ , used earlier in the context of the wave-function of the  $\eta'$ -meson, and  $n_f$  in the  $\beta$ -function; the former reflects the quark content of the SU(3) flavour-singlet meson, while the latter is the number of the active quarks, which (together with the gluons) determine the renormalization effects in the LCDAs of the  $\eta'$ -meson, probed at a virtuality  $Q^2$ . The discussion of these anomalous dimensions in the one- and two-loop accuracy can be found in Ref. [22]. Our choice of the constant prefactor in the gluonic matrix element (21) is reflected in the non-diagonal anomalous dimensions presented above.

The anomalous dimensions (39) also define the quantities  $\rho_n^{(g)}$  and  $\rho_n^{(q)}$  entering in the Gegenbauer moments (36) and (37) as follows:

$$\rho_n^{(q)} = 6 \frac{\gamma_+^n - \gamma_{QQ}^n}{\gamma_{QG}^n}, \quad \rho_n^{(g)} = \frac{1}{6} \frac{\gamma_{QG}^n}{\gamma_-^n - \gamma_{QQ}^n}. \quad (40)$$

The prefactor in the gluonic light-cone DA (35) is chosen as  $u^2 \bar{u}^2$  according to Ref. [3], which accounts for the appearance of the factor  $u\bar{u}$  in the denominator of the integral function in the gluonic matrix element (28). Such a functional dependence is also in agreement with the general expression for the ‘‘asymptotic’’ form of the LCDAs resulting from the conformal symmetry [10, 12].

We use an approximate form for the  $\eta'$ -meson light-cone wave-function in which only the first non-asymptotic term in both the quark-antiquark and gluonic DAs is kept. Thus,

$$\phi_{\eta'}^{(q)}(u, Q^2) = 6u\bar{u} [1 + 6(1 - 5u\bar{u}) A_2(Q^2)], \quad \phi_{\eta'}^{(g)}(u, Q^2) = 5u^2 \bar{u}^2 (u - \bar{u}) B_2(Q^2), \quad (41)$$

where the explicit forms of the Gegenbauer polynomials  $C_2^{3/2}(u - \bar{u})$  and  $C_1^{5/2}(u - \bar{u})$  have been used. The free parameters  $B_2^{(q)}(\mu_0^2)$  and  $B_2^{(g)}(\mu_0^2)$  (the Gegenbauer coefficients), which enter in the Gegenbauer moments  $A_2(Q^2)$  and  $B_2(Q^2)$ , are not determined from

first principles and have to be modeled or extracted from a phenomenological analysis of experimental data. We defer the quantitative discussion of these Gegenbauer coefficients to Sec. 4.

There is an additional point concerning the scale  $\mu_0^2$ . The usual choice of the scale  $\mu_0^2 = 1 \text{ GeV}^2$  made in the analysis of the pion form factor and the  $\pi^0 - \gamma$  transition form factor represents the initial value for the evolution of the LCDAs. As the mass of the  $\eta'$ -meson is of order 1 GeV, a more realistic choice of the parameter  $\mu_0^2$  is  $\mu_0^2 = 2 \text{ GeV}^2$ , which we shall adopt. Consistent with this assumption, and with the choice  $Q^2 = |q^2| + m_{\eta'}^2$ , where  $q^2$  is the total gluon virtuality in the  $\eta' g^* g^*$  vertex, we shall also set  $Q_0^2 = 2 \text{ GeV}^2$  in the calculation of the perturbative kernel.

### 3 The $\eta' g^* g^*$ Effective Vertex Function

In the momentum space, the effective  $\eta' g^* g^*$  vertex can be extracted from the invariant matrix element of the process  $\eta' \rightarrow g^* g^*$  with the help of the relation<sup>6</sup>:

$$\mathcal{M} = \mathcal{M}^{(q)} + \mathcal{M}^{(g)} \equiv F_{\eta' g^* g^*}(q_1^2, q_2^2, m_{\eta'}^2) \delta_{AB} \varepsilon^{\mu\nu\rho\sigma} \varepsilon_{1\mu}^{A*} \varepsilon_{2\nu}^{B*} q_{1\rho} q_{2\sigma}, \quad (42)$$

where  $\mathcal{M}^{(q)}$  and  $\mathcal{M}^{(g)}$  are the contributions from the quark-antiquark and gluonic components of the  $\eta'$ -meson, respectively, and  $q_i$  and  $\varepsilon_i^A$  ( $i = 1, 2$ ) are the four-momenta and the polarization vectors of the final virtual gluons. The four-momentum of the  $\eta'$ -meson is related to the four-momenta of the gluons by energy-momentum conservation:  $p_\mu = q_{1\mu} + q_{2\mu}$ . The individual contributions  $\mathcal{M}^{(q)}$  and  $\mathcal{M}^{(g)}$  to the invariant amplitude (42) can be calculated by using the  $\eta'$ -meson projection operators onto the quark-antiquark (18) and the two-gluonic (32) states, yielding

$$\mathcal{M}^{(q)} = i f_{\eta'} \int_0^1 du \phi_{\eta'}^{(q)}(u, Q^2) \mathcal{P}_{j\beta b; i\alpha a}^{(q)} \delta^{ab} [T_H^{(q)}]_{ij}^{\alpha\beta}, \quad (43)$$

$$\mathcal{M}^{(g)} = \frac{i f_{\eta'}}{2} \int_0^1 du \frac{\phi_{\eta'}^{(g)}(u, Q^2)}{u\bar{u}} \mathcal{P}_{\sigma D; \rho C}^{(g)} [T_H^{(g)}]_{CD}^{\rho\sigma}, \quad (44)$$

where  $T_H^{(q)}$  and  $T_H^{(g)}$  are the quark-antiquark and gluonic hard-scattering kernels calculated in the perturbative QCD, respectively. The factor 1/2 in Eq. (44) takes into account the two identical gluons in the  $\eta'$ -meson. To go further, it is necessary to define the light-like vector  $n_\mu$  appearing in the individual invariant amplitudes (43) and (44) in terms of the physical vectors of the problem under study.

#### 3.1 Specifying the Light-Like Vector $n_\mu$

We now proceed to express the vector  $n_\mu$  in terms of the gluon momenta  $q_{1\mu}$  and  $q_{2\mu}$  in the  $\eta' g^* g^*$  vertex. In particular, we consider the case when both the gluons are off the

---

<sup>6</sup>The difference in the phase factor  $i$  between the definition of the effective  $\eta' g^* g^*$  vertex function in this paper and in Ref. [2] is related to the corresponding difference in the definitions of the projection operators of the  $\eta'$ -meson onto the quark-antiquark and gluonic states.

mass shell and have virtualities  $q_1^2$  and  $q_2^2$  comparable to the  $\eta'$ -meson mass squared.

Let us assume, to be definite, that the virtualities of both gluons are time-like ( $q_1^2 > 0$  and  $q_2^2 > 0$ ). In that case, the two light-like vectors  $n_\mu^{(+)}$  and  $n_\mu^{(-)}$  can be constructed from  $q_{1\mu}$  and  $q_{2\mu}$  (or, equivalently, from  $p_\mu = q_{1\mu} + q_{2\mu}$  and  $q_{2\mu}$ ):

$$n_\mu^{(\pm)} = C_n \left\{ 2q_2^2 p_\mu + \left[ q_1^2 - q_2^2 - m_{\eta'}^2 \pm \lambda_K \left( m_{\eta'}, \sqrt{q_1^2}, \sqrt{q_2^2} \right) \right] q_{2\mu} \right\}, \quad (45)$$

where  $C_n$  is an arbitrary factor and  $\lambda_K(a, b, c)$  is a kinematic function, defined as follows:

$$\lambda_K(a, b, c) = \sqrt{(a+b+c)(a-b-c)(a-b+c)(a+b-c)}. \quad (46)$$

In the limit of neglecting the  $\eta'$ -meson mass (i.e., setting  $m_{\eta'} = 0$ ), these vectors are simplified to:

$$n_\mu^{(\pm)} = C_n \left\{ 2q_2^2 p_\mu + [q_1^2 - q_2^2 \pm |q_1^2 - q_2^2|] q_{2\mu} \right\}, \quad (47)$$

as  $\lambda_K(0, \sqrt{q_1^2}, \sqrt{q_2^2}) = |q_1^2 - q_2^2|$ . Thus, if  $q_1^2 > q_2^2$ , then these vectors have the forms:

$$\begin{aligned} n_\mu^{(+)} &= 2C_n (q_2^2 q_{1\mu} + q_1^2 q_{2\mu}), \\ n_\mu^{(-)} &= 2C_n q_2^2 p_\mu, \end{aligned} \quad (48)$$

while for  $q_1^2 < q_2^2$  they are:

$$\begin{aligned} n_\mu^{(-)} &= 2C_n (q_2^2 q_{1\mu} + q_1^2 q_{2\mu}), \\ n_\mu^{(+)} &= 2C_n q_2^2 p_\mu. \end{aligned} \quad (49)$$

If we take  $n_\mu = n_\mu^{(+)}$  ( $n_\mu = n_\mu^{(-)}$ ), then in the limit  $m_{\eta'} = 0$ , the light-like vector  $P_\mu$  (29) vanishes for  $q_1^2 < q_2^2$  ( $q_1^2 > q_2^2$ ) and, hence, the projection operators onto the quark-antiquark (18) and gluonic (32) states also vanish. To get non-vanishing projection operators in both regions, the vector  $n_\mu$  should be taken as:

$$n_\mu = n_\mu^{(+)} \Theta(q_1^2 - q_2^2) + n_\mu^{(-)} \Theta(q_2^2 - q_1^2), \quad (50)$$

where  $\Theta(x)$  is the unit step function. To write this vector uniformly, it is convenient to introduce the total gluon virtuality  $q^2$ , the asymmetry parameter  $\omega$ , and the relative  $\eta'$ -meson mass squared  $\eta$  as follows:

$$q^2 = q_1^2 + q_2^2, \quad \omega = \frac{q_1^2 - q_2^2}{q^2}, \quad \eta = \frac{m_{\eta'}^2}{q^2}. \quad (51)$$

If we also redefine the factor  $C_n$  as  $C_n = \tilde{C}_n/q^2$ , the vector  $n_\mu$  (50) can be rewritten in the form:

$$n_\mu = \tilde{C}_n [(1 - \omega) p_\mu + (\omega - \eta + \omega\lambda) q_{2\mu}], \quad (52)$$

where the function  $\lambda$  can be written as<sup>7</sup>:

$$\lambda = \sqrt{1 - \frac{2\eta}{\omega^2} + \frac{\eta^2}{\omega^2}}. \quad (53)$$

---

<sup>7</sup>Note,  $\lambda_K$  and  $\lambda$  are different functions.

In the massless limit of the  $\eta'$ -meson ( $\eta = 0$ ),  $\lambda = 1$ . With this specification of the light-like vector  $n_\mu$ , its scalar product with the  $\eta'$ -meson four-momentum  $p_\mu$  is:

$$(pn) = -\frac{q^2}{2} \tilde{C}_n \omega \lambda (\omega - \eta + \omega \lambda), \quad (54)$$

which allows us to write the light-like vector  $P_\mu$  (29) in the following form:

$$P_\mu = \frac{1}{2\omega\lambda} [(\omega - \eta + \omega \lambda) p_\mu + 2\eta q_{2\mu}]. \quad (55)$$

With this, the Lorentz structure in the projection operator (32) is reduced to the form:

$$\frac{\varepsilon_{\mu\nu\rho\sigma} n^\rho p^\sigma}{(np)} = \frac{2}{\omega\lambda} \frac{\varepsilon_{\mu\nu\rho\sigma} q_1^\rho q_2^\sigma}{q^2} = \frac{2}{\lambda} \frac{\varepsilon_{\mu\nu\rho\sigma} q_1^\rho q_2^\sigma}{q_1^2 - q_2^2}. \quad (56)$$

Note that both the vector  $P_\mu$ , defining the Dirac structure of the  $\eta'$ -meson projection operator onto the quark-antiquark state (18), and the Lorentz structure considered above, which comes from the projection operator onto the gluonic state (18), are independent of the choice of the factor  $\tilde{C}_n$ .

For the case when both the gluons have space-like virtualities ( $q_1^2 < 0$  and  $q_2^2 < 0$ ), the same set of quantities can be introduced as in Eq. (51), with the obvious difference that the total gluon virtuality and the relative  $\eta'$ -meson mass squared are negative. This difference does not change the result obtained for the time-like gluon virtualities and, thus, Eqs. (52), (55) and (56) are valid in this case also.

### 3.2 The Quark Part of the $\eta' g^* g^*$ Vertex

The light-like vector  $P_\mu$ , and hence the  $\eta'$ -meson projection operator (18) onto the quark-antiquark state, is completely defined in terms of the physical vectors – the four-momenta of the gluons. Hence, we can calculate the quark part of the  $\eta' g^* g^*$  effective vertex function starting from the invariant amplitude (43), obtaining the hard-scattering kernel:

$$[T_H^{(q)}]^{\alpha\beta} = V_{\mu\nu}^{\alpha\beta;AB}(up, \bar{u}p, -q_1, -q_2) \varepsilon_{1\mu}^{A*} \varepsilon_{2\nu}^{B*}, \quad (57)$$

where the Dirac indices  $i$  and  $j$  are not shown explicitly; the exact expression for the effective quark-antiquark-gluon-gluon vertex in the lowest order in perturbative QCD can be found in Eq. (3.3) of Ref. [2]. This yields the following result:

$$\mathcal{M}^{(q)} = -\frac{if_{\eta'} \sqrt{N_f}}{4N_c} 4\pi\alpha_s(Q^2) \delta_{AB} \int_0^1 du \phi_{\eta'}^{(q)}(u, Q^2) \text{Sp} \left\{ \gamma_5 (P\gamma) \frac{(\varepsilon_1^{A*} \gamma)([up - q_2] \gamma)(\varepsilon_2^{B*} \gamma)}{(up - q_2)^2 + i\epsilon} \right\}, \quad (58)$$

where  $Q^2 = |q^2| + m_{\eta'}^2$  and the summation over the quark colour and flavour indices have been performed. This matrix element contains the contributions from both diagrams presented in Fig. 1, as the contribution from the second diagram can be transformed to the form of the first one with the help of the symmetry property of the quark-antiquark light-cone DA:  $\phi_{\eta'}^{(q)}(u, Q^2) = \phi_{\eta'}^{(q)}(\bar{u}, Q^2)$ . It is easy to see that the parameter  $C$  defined by

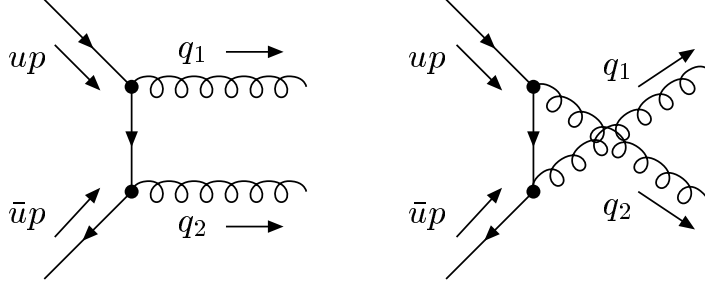


Figure 1: Leading Feynman diagrams contributing to the quark part of the  $\eta'g^*g^*$  vertex.

Eq. (2.3) of Ref. [2] is connected with the  $\eta'$ -meson decay constant  $f_{\eta'}$  used here by the following relation:  $C = \sqrt{N_f} f_{\eta'}$ .

Taking all this into account as well as the Ansatz (42) for extracting the  $\eta'g^*g^*$  effective vertex function, the result for the quark part can be written as follows:

$$F_{\eta'g^*g^*}^{(q)}(q^2, \omega, \eta) = \frac{4\pi\alpha_s(Q^2)}{q^2} \frac{f_{\eta'}\sqrt{N_f}}{N_c\omega\lambda} \int_0^1 du \phi_{\eta'}^{(q)}(u, Q^2) \frac{\omega(1+\lambda) + \eta(u-\bar{u})}{1 + \omega(u-\bar{u}) - 2u\bar{u}\eta + i\epsilon}. \quad (59)$$

The quark-antiquark contribution, in the approximation of keeping the first two terms in the corresponding distribution amplitude  $\phi_{\eta'}^{(q)}(u, Q^2)$  [see Eq. (41)], can be conveniently written in the following form (similar to Eq. (3.7) of Ref. [2]):

$$F_{\eta'g^*g^*}^{(q)}(q^2, \omega, \eta) = \frac{4\pi\alpha_s(Q^2)}{m_{\eta'}^2\lambda} \frac{3f_{\eta'}\sqrt{N_f}}{N_c} \left\{ G_0^{(q)}(\omega, \eta) + 6A_2(Q^2)G_2^{(q)}(\omega, \eta) \right\}, \quad (60)$$

where  $A_2(Q^2)$  is the Gegenbauer moment defined by Eq. (36), and the functions  $G_0^{(q)}(\omega, \eta)$  and  $G_2^{(q)}(\omega, \eta)$  are:

$$G_0^{(q)}(\omega, \eta) = 1 - \lambda + \left[ 1 - \frac{\omega^2}{\eta}(1 - \lambda) \right] \left[ \frac{1}{2\omega} \ln \left| \frac{1 + \omega}{1 - \omega} \right| + \lambda J(\omega, \eta) \right], \quad (61)$$

$$G_2^{(q)}(\omega, \eta) = \frac{5}{2\eta} \left\{ \frac{\omega^2}{\eta}(1 - \lambda)^2 - \left( 1 - \frac{\eta}{15} \right) (1 - \lambda) \right. \\ \left. - \left[ 1 - \frac{\omega^2}{\eta}(1 - \lambda) \right] \left[ 1 - \frac{2\eta}{5} - \frac{\omega^2}{\eta}(1 - \lambda) \right] \left[ \frac{1}{2\omega} \ln \left| \frac{1 + \omega}{1 - \omega} \right| + \lambda J(\omega, \eta) \right] \right\}. \quad (62)$$

The results given above are presented using the function:

$$J(\omega, \eta) \equiv \int_0^1 \frac{du}{1 + \omega(u - \bar{u}) - 2u\bar{u}\eta + i\epsilon}, \quad (63)$$

whose explicit form and the asymptotic behaviour can be found in Appendix B of Ref. [2].

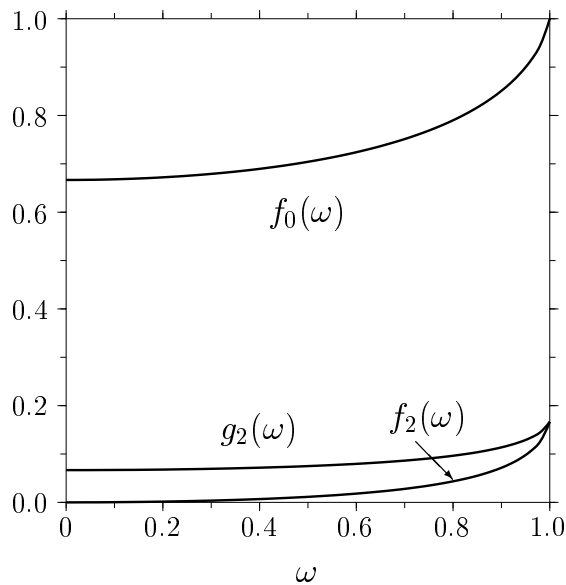


Figure 2: The functions  $f_0(\omega)$ ,  $f_2(\omega)$ , and  $g_2(\omega)$  describing the large  $|q^2|$  asymptotic behaviour of the  $\eta'g^*g^*$  effective vertex function, with the virtualities of the gluons having same signs.

When the  $\eta'$ -meson mass is negligible in comparison with the total gluon virtuality  $|q^2|$  (i.e., in the limit of small  $\eta$ ), Eq. (60) reduces to:

$$F_{\eta'g^*g^*}^{(q)}(q^2, \omega, 0) = \frac{4\pi\alpha_s(|q^2|)}{q^2} \frac{3f_{\eta'}\sqrt{N_f}}{N_c} \{f_0(\omega) + 6A_2(|q^2|)f_2(\omega)\}, \quad (64)$$

(in accordance with Eq. (3.10) of Ref. [2]) as the functions  $G_0^{(q)}(\omega, \eta)$  and  $G_2^{(q)}(\omega, \eta)$  presented above are dominated by the term  $G_i^{(q)}(\omega, \eta) \simeq \eta f_i(\omega)$  in this limit, and the functions  $f_i(\omega)$  ( $i = 0, 2$ ) are defined as follows:

$$f_0(\omega) = \frac{1}{\omega^2} \left[ 1 - \frac{1 - \omega^2}{2\omega} \ln \frac{1 + \omega}{1 - \omega} \right], \quad (65)$$

$$f_2(\omega) = \frac{1}{12\omega^2} [3(5 - \omega^2) f_0(\omega) - 10]. \quad (66)$$

The dependence of these functions on the asymmetry parameter  $\omega$  is presented in Fig. 2. The asymmetry parameter is defined in the interval  $-1 \leq \omega \leq 1$ , but as the functions  $f_0(\omega)$  and  $f_2(\omega)$  are symmetric, it is sufficient to present them in the region of positive values of the argument.

If one of the gluons is on the mass shell, for example, the second one ( $q_2^2 = 0$ ), the asymmetry parameter  $\omega = 1$ ,  $\lambda = 1 - \eta$ , and it is easy to get from Eq. (59) the following result:

$$F_{\eta'g^*g}^{(q)}(q_1^2, 0, m_{\eta'}^2) = \frac{4\pi\alpha_s(Q^2)}{q_1^2 - m_{\eta'}^2} \frac{f_{\eta'}\sqrt{N_f}}{N_c} \int_0^1 \frac{du}{u} \phi_{\eta'}^{(q)}(u, Q^2). \quad (67)$$

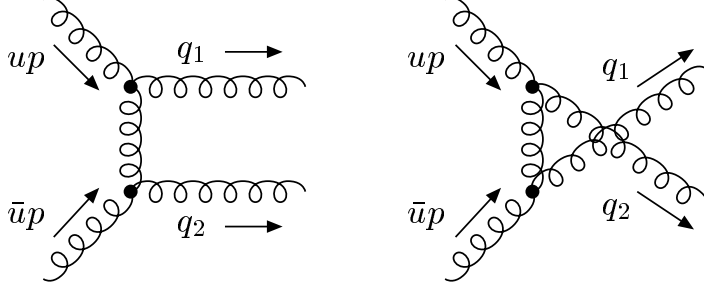


Figure 3: Leading order contribution to the gluonic part of the  $\eta'g^*g^*$  vertex.

In the approximation of the  $\eta'$ -meson DAs adopted here, the first inverse moment of the quark-antiquark twist-two DA is:

$$\int_0^1 \frac{du}{u} \phi_{\eta'}^{(g)}(u, Q^2) = 3 [1 + A_2(Q^2)]. \quad (68)$$

Thus, in this case, the  $\eta'g^*g$  effective vertex function is defined by the first inverse moment of the  $\eta'$ -meson quark-antiquark DA and it has a pole form, with the pole being at  $q_1^2 = m_{\eta'}^2$ . Of course, this result is not supposed to be used in the vicinity of the singular point  $q_1^2 \simeq m_{\eta'}^2$ ; the perturbative form sets in at a higher value of  $q_1^2$ , typically  $q_1^2 \simeq 2 \text{ GeV}^2$ . Also, as discussed in Ref. [2], this pole behaviour results from ignoring the transverse momentum in the definition of the  $\eta'$ -meson wave-function and, hence, is not physical.

### 3.3 The Gluonic Part of the $\eta'g^*g^*$ Vertex

The gluonic part of the  $\eta'g^*g^*$  vertex function originates from the diagrams presented in Fig. 3. To calculate this effective vertex function with the help of the invariant amplitude (44), the corresponding hard-scattering kernel  $T_{\text{H}}^{(g)}$  can be obtained from the effective four-gluon vertex  $V_{\mu\nu\rho\sigma}^{ABCD}(q_1, q_2, q_3, q_4)$ , which is defined in Eq. (4.3) of Ref. [2], as follows:

$$[T_{\text{H}}^{(g)}]_{\rho\sigma}^{CD} = V_{\mu\nu\rho\sigma}^{ABCD}(-q_1, -q_2, up, \bar{u}p) \varepsilon_{1\mu}^{A*} \varepsilon_{2\nu}^{B*}. \quad (69)$$

Substituting Eq. (56) into Eq. (32), the  $\eta'$ -meson projection operator onto the two-gluon state, the invariant matrix element (44) can be rewritten in the form:

$$\mathcal{M}^{(g)} = -\frac{f_{\eta'}}{4N_c \sqrt{N_f} \lambda} \int_0^1 du \frac{\phi_{\eta'}^{(g)}(u, Q^2)}{u\bar{u}} \frac{\varepsilon^{\rho\sigma\lambda\tau} q_{1\lambda} q_{2\tau}}{q_1^2 - q_2^2} \delta_{CD} [T_{\text{H}}^{(g)}]_{\rho\sigma}^{CD}, \quad (70)$$

where the parameter  $\lambda$  is defined in Eq. (53). Comparison of this matrix element with the one given in Eq. (4.1) of Ref. [2], with  $C = f_{\eta'} \sqrt{N_f}$ , shows that the two expressions differ by the factor  $Q^2/[2N_f \lambda (q_1^2 - q_2^2)] = Q^2/(2N_f \lambda \omega q^2)$ . Note also the difference in the factor  $i$  in the definitions of the gluonic projection operators in this paper and in Ref. [2]



(this difference then also reflects itself in the definition of the quark-antiquark projection operator). We have now understood this mismatch, related to two errors made in Ref. [2]: First, the factor 1/2 is due to the identity of gluons in the  $\eta'$ -meson, which was missed in Ref. [2]; Second, the factor  $Q^2/(q_1^2 - q_2^2)$  is required by the Bose symmetry of the final gluons in the process  $\eta' \rightarrow g^*g^*$  described by this amplitude, also overlooked in Ref. [2]. Finally, the parameter  $\lambda$  in the denominator of  $\mathcal{M}^{(g)}$  enters as we now take into account the  $\eta'$ -meson mass;  $\lambda = 1$  for the case of the massless  $\eta'$ -meson. Taking into account the difference between Eq. (70) in this paper and Eq. (4.1) of Ref. [2] pointed above, the corrected result for the gluonic part of the  $\eta'g^*g^*$  effective vertex function can be obtained from Eqs. (4.7) and (4.8) of Ref. [2], which now reads as follows:

$$F_{\eta'g^*g^*}^{(g)}(q^2, \omega, \eta) = -\frac{4\pi\alpha_s(Q^2)}{m_{\eta'}^2\lambda} \frac{5f_{\eta'}}{2\sqrt{N_f}} B_2(Q^2) G_2^{(g)}(\omega, \eta), \quad (71)$$

where the Gegenbauer moment  $B_2(Q^2)$  is defined in Eq. (41), and the function  $G_2^{(g)}(\omega, \eta)$  has the form:

$$\begin{aligned} G_2^{(g)}(\omega, \eta) &= \frac{2\eta}{\omega} \int_0^1 du u\bar{u} (u - \bar{u}) \frac{\eta + \omega(u - \bar{u})}{1 + \omega(u - \bar{u}) - 2u\bar{u}\eta + i\epsilon} \\ &= \frac{5}{3} + \frac{2}{\eta} - \frac{4\omega^2}{\eta^2} + \frac{1}{2\omega} \left[1 - \frac{\omega^2}{\eta}\right] \left[1 - \frac{4\omega^2}{\eta^2}\right] \ln \left| \frac{1 + \omega}{1 - \omega} \right| \\ &+ \eta \left[1 - \frac{2}{\eta} - \frac{2 + \omega^2}{\eta^2} + \frac{8\omega^2}{\eta^3} - \frac{4\omega^4}{\eta^4}\right] J(\omega, \eta). \end{aligned} \quad (72)$$

This function is symmetric in its first argument under the change  $\omega \rightarrow -\omega$ :  $G_2^{(g)}(-\omega, \eta) = G_2^{(g)}(\omega, \eta)$ , in accordance with the requirement of the Bose symmetry for the  $\eta'g^*g^*$  vertex.

In the limit of the large total gluon virtuality ( $|q^2| \gg m_{\eta'}^2$ ), the gluonic part of the  $\eta'g^*g^*$  effective vertex function simplifies and can be expressed as follows:

$$F_{\eta'g^*g^*}^{(g)}(q^2, \omega, 0) = -\frac{4\pi\alpha_s(|q^2|)}{q^2} \frac{5f_{\eta'}}{2\sqrt{N_f}} B_2(|q^2|) g_2(\omega), \quad (73)$$

where the function  $g_2(\omega)$  has the form:

$$g_2(\omega) = \frac{3f_0(\omega) - 2}{6\omega^2}. \quad (74)$$

Here,  $f_0(\omega)$  is the function defined in Eq. (65). Note that the function  $g_2(\omega)$  is symmetric under the exchange  $\omega \rightarrow -\omega$ :  $g_2(-\omega) = g_2(\omega)$ , in agreement with the observation made in Ref. [3]. At  $\omega = 0$  it has a non-vanishing value:  $g_2(0) = 1/15$ , and at the end points,  $\omega = \pm 1$ , it has the value  $g_2(\pm 1) = 1/6$ . The explicit dependence of  $g_2(\omega)$  on the asymmetry parameter  $\omega$  is presented in Fig. 2.

If one of the gluons is on the mass shell, say, the second gluon ( $q_2^2 = 0$ ), the gluonic part of the  $\eta'g^*g$  effective vertex function can be written in the following form:

$$F_{\eta'g^*g}^{(g)}(q_1^2, 0, m_{\eta'}^2) = -\frac{4\pi\alpha_s(Q^2)}{q_1^2 - m_{\eta'}^2} \frac{5f_{\eta'}}{2\sqrt{N_f}} B_2(Q^2) G_2^{(g)}(1, \eta), \quad (75)$$

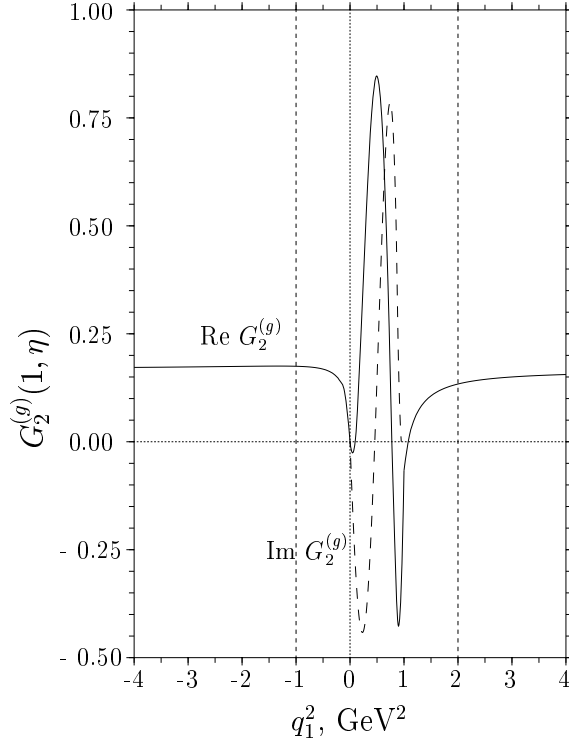


Figure 4: The real (solid curve) and imaginary (long-dashed curve) parts of the function  $G_2^{(g)}(1, \eta)$ , where  $\eta = m_{\eta'}^2/q_1^2$ , as a function of the momentum squared  $q_1^2$  of the virtual gluon. The vertical short-dashed lines, drawn at  $q_1^2 = -1 \text{ GeV}^2$  and  $q_1^2 = 2 \text{ GeV}^2$ , demarcate the regions of applicability of the perturbative results, which are to the left and right of these lines for the space-like and time-like gluon virtualities, respectively.

where  $\eta = m_{\eta'}^2/q_1^2$ , the value  $\lambda = 1 - \eta$  was taken into account at  $\omega = 1$ , and the function  $G_2^{(g)}(1, \eta)$  is:

$$G_2^{(g)}(1, \eta) = \frac{5}{3\eta} + \frac{2}{\eta^2} - \frac{4}{\eta^3} - \frac{1}{\eta} \left[ 1 - \frac{1}{\eta} \right] \left[ 1 - \frac{4}{\eta^2} \right] \ln(1 - \eta). \quad (76)$$

The dependence of this function on the gluon virtuality  $q_1^2$  is presented in Fig. 4 with the value  $G_2^{(g)}(1, 0) = 1/6$  corresponding to the large  $q_1^2$  asymptotics. In line with the quark-antiquark part (67) of the  $\eta'g^*g$  effective vertex function, the gluonic part (75) has the same pole behaviour at  $q_1^2 = m_{\eta'}^2$ .

To conclude this section, we present the expression for the  $\eta'g^*g^*$  effective vertex function resulting from the perturbative QCD analysis. Combining the quark-antiquark (60) and the gluonic (71) parts of the  $\eta'g^*g^*$  effective vertex function, the perturbative result for the vertex can be expressed as follows:

$$F_{\eta'g^*g^*}(q_1^2, q_2^2, m_{\eta'}^2) = \frac{4\pi\alpha_s(Q^2)}{m_{\eta'}^2\lambda} \sqrt{3}f_{\eta'} \quad (77)$$

$$\times \left[ G_0^{(q)}(\omega, \eta) + 6A_2(Q^2)G_2^{(q)}(\omega, \eta) - \frac{5}{6}B_2(Q^2)G_2^{(g)}(\omega, \eta) \right],$$

where the total gluon virtuality is  $q^2 = q_1^2 + q_2^2$ , the variables  $\omega$  and  $\eta$  on the right-hand side are defined in Eq. (51), and  $Q^2 = |q^2| + m_{\eta'}^2$ . Being a perturbative-QCD result, this expression is valid in the large  $|q^2|$  region.

As mentioned above, both the quark-antiquark (67) and the gluonic (75) parts of the  $\eta' - g$  transition form factor have the phenomenological form (1) which allows to extract the slowly varying function  $H(q_1^2, 0, m_{\eta'}^2)$ :

$$H(q_1^2, 0, m_{\eta'}^2) = \frac{4\pi\alpha_s(Q^2)}{m_{\eta'}^2} \sqrt{3} f_{\eta'} \left[ 1 + A_2(Q^2) - \frac{5}{6} B_2(Q^2) G_2^{(g)}(1, \eta) \right]. \quad (78)$$

The non-trivial dependence on the  $\eta'$ -meson mass is coming through the function  $G_2^{(g)}(1, \eta)$ , with  $\eta = m_{\eta'}^2/q_1^2$ , which is to be traced back to the gluonic component of the  $\eta'$ -meson.

## 4 Numerical Analysis

As demonstrated earlier, the correction due to the mass of the  $\eta'$ -meson appears already in the leading-twist (twist-two) light-cone approximation. It is of interest to know numerically the effect of including the  $\eta'$ -meson mass in the  $\eta' g^* g^*$  effective vertex function. To work this out, we need to specify the input values for the various parameters. To that end, we note that the  $\eta'$ -meson decay constant can be related with the flavour-singlet decay constant  $f_1 \simeq 1.17 f_\pi$ , where  $f_\pi = 133$  MeV is the  $\pi$ -meson decay constant, as:  $f_{\eta'} = f_1 \cos \theta_1$  with the mixing angle  $\theta_1 \simeq -9.2^\circ$  [23]. With this, it is easy to check that  $f_{\eta'} \simeq 2f_\pi/\sqrt{3}$ . In estimations of the effective vertex function, the strong coupling  $\alpha_s(Q^2)$  is used in the two-loop approximation with the QCD scale parameter  $\Lambda_{\overline{\text{MS}}}^{(4)} = 305$  MeV corresponding to four active flavours ( $n_f = 4$ ). The central values of the  $c$ - and  $b$ -quark  $\overline{\text{MS}}$  masses,  $\bar{m}_c = 1.3$  GeV and  $\bar{m}_b = 4.3$  GeV [24], were used for the separation of regions with different active-quark flavours in the strong coupling  $\alpha_s(Q^2)$ . In this context we also specify the constrained parameters (38) and (40) in the  $\eta'$ -meson DAs:  $\gamma_+^2 \simeq -0.645$ ,  $\gamma_-^2 \simeq -1.421$ ,  $\rho_2^{(q)} \simeq 2.863$ , and  $\rho_2^{(g)} \simeq -0.010$ , calculated for  $n_f = 4$ . For the starting point of the evolution scale we take  $\mu_0^2 = Q_0^2 = 2$  GeV<sup>2</sup>. We do not include errors on these parameters, as they are relatively small.

The largest uncertainty in the  $\eta' g^* g^*$  effective vertex function is due to the gluonic Gegenbauer moment  $B_2(Q^2)$  (37). In particular, in the approximation (41), a fit to the CLEO and L3 data on the  $\eta' - \gamma$  transition form factor for  $Q^2$  larger than 2 GeV<sup>2</sup> was recently undertaken in Ref. [3], yielding

$$A_2(1 \text{ GeV}^2) = -0.08 \pm 0.04, \quad B_2(1 \text{ GeV}^2) = 9 \pm 12, \quad (79)$$

where, in the analysis in Ref. [3], the initial scale in the evolution of the Gegenbauer moments was taken as  $\mu_0^2 = 1$  GeV<sup>2</sup>. The estimates (79) can be translated in terms of the universal free parameters  $B_2^{(q)}(\mu_0^2)$  and  $B_2^{(g)}(\mu_0^2)$  (the Gegenbauer coefficients), fixed at the same initial scale  $\mu_0^2$  of the DA evolution, yielding:

$$B_2^{(q)}(1 \text{ GeV}^2) = 0.02 \pm 0.17, \quad B_2^{(g)}(1 \text{ GeV}^2) = 9.0 \pm 11.5. \quad (80)$$

We note that this analysis of the  $\eta' - \gamma$  transition form factor yields an order of magnitude uncertainty in these parameters, taking into account the  $\pm 1\sigma$  error. In addition, the Gegenbauer moments  $A_2(1 \text{ GeV}^2)$  and  $B_2(1 \text{ GeV}^2)$  are strongly correlated and we refer to Fig. 3 of Ref. [3] where the correlation between these quantities is presented.

The other process which allows to get an independent information on the Gegenbauer coefficients in the  $\eta'g^*g$  vertex is the inclusive decay  $\Upsilon(1S) \rightarrow \eta'X$ . Recently the  $\eta'$ -meson energy spectrum was measured in this process by the CLEO collaboration and presented in Ref. [8]. The CLEO data prefers the perturbative-QCD motivated form of the  $\eta' - g$  transition form factor (1) for the hard part of the  $\eta'$ -meson energy spectrum,  $E_{\eta'} > 0.35M_\Upsilon$ , where  $M_\Upsilon = 9.46 \text{ GeV}$  is the mass of the  $\Upsilon(1S)$ -resonance. Based on this observation, the form (78) for the function  $H(q_1^2, 0, m_{\eta'}^2)$  resulting from the hard-scattering perturbative-QCD approach for the  $\eta'g^*g$  effective vertex function was adopted by us in Ref. [9], obtaining independent constraints on the Gegenbauer coefficients. Unfortunately, the CLEO data on the decay  $\Upsilon(1S) \rightarrow \eta'X$  is statistically very uncertain for the end part of the  $\eta'$ -meson energy spectrum, leaving large uncertainties in the determination of the Gegenbauer coefficients from this process alone. The combined fit to the data from the  $\eta' - \gamma$  transition form factor and the  $\Upsilon(1S) \rightarrow \eta'X$  decay leads to more restrictive constraints on these coefficients which we have presented and discussed in detail in Ref. [9]. The combined best fit of the Gegenbauer coefficients and the Gegenbauer moments yields the following ( $\pm 1\sigma$ ) values, respectively [9]:

$$\begin{aligned} B_2^{(q)}(\mu_0^2) &= -0.008 \pm 0.054, & B_2^{(g)}(\mu_0^2) &= 4.6 \pm 2.5, \\ A_2(\mu_0^2) &= -0.054 \pm 0.029, & B_2(\mu_0^2) &= 4.6 \pm 2.7, \end{aligned} \quad (81)$$

where the starting point of the evolution in the  $\eta'$ -meson DAs is taken as  $\mu_0^2 = 2 \text{ GeV}^2$ .

The predictions for the  $\eta'g^*g$  effective vertex function  $F_{\eta'g^*g}(q_1^2, 0, m_{\eta'}^2)$ , with the second gluon on the mass shell ( $q_2^2 = 0$ ), are presented in Fig. 5 for the time-like (left frame) and space-like (right frame) virtuality  $q_1^2$  of the off-shell gluon. The labels on the curves C, LL, and UR correspond to the central, lower-left, and upper-right points of the combined best fit of the Gegenbauer coefficients presented in Fig. 5 of Ref. [9]; their values can also be read from Eq. (81). We note that the effect of including the  $\eta'$ -meson mass in the vertex function is significant; it becomes crucial for the time-like gluon virtuality in the region  $q_1^2 \lesssim 5 \text{ GeV}^2$  for the upper-right part of the combined best-fit region of the Gegenbauer coefficients (the curves labeled as UR), but also to a lesser extent for the central values of the fit parameters (the curves labeled as C). For the space-like gluon virtuality the  $\eta'$ -meson mass effect is numerically not so strong. Nevertheless, it decreases the absolute value of the  $\eta'g^*g$  transition form factor by approximately 10 percent in the region of small gluon virtualities ( $|q_1^2| \lesssim 5 \text{ GeV}^2$ ) for the Gegenbauer coefficients from the lower-left part of the combined best-fit region (denoted by the curves labeled as LL) and for the central values of the fit (the curves labeled C).

Summarizing this section, the results presented in Eqs. (77) and (78) (to be read with Eq. (1)) are our principal analytic results for the vertex functions  $F_{\eta'g^*g^*}(q_1^2, q_2^2, m_{\eta'}^2)$  and  $F_{\eta'g^*g}(q_1^2, 0, m_{\eta'}^2)$ , respectively. The vertex function  $F_{\eta'g^*g}(q_1^2, 0, m_{\eta'}^2)$  is displayed numerically in Fig. 5 in the space-like and time-like regions of the gluon virtuality, based on perturbative QCD and our current knowledge of the Gegenbauer coefficients. Inclusion

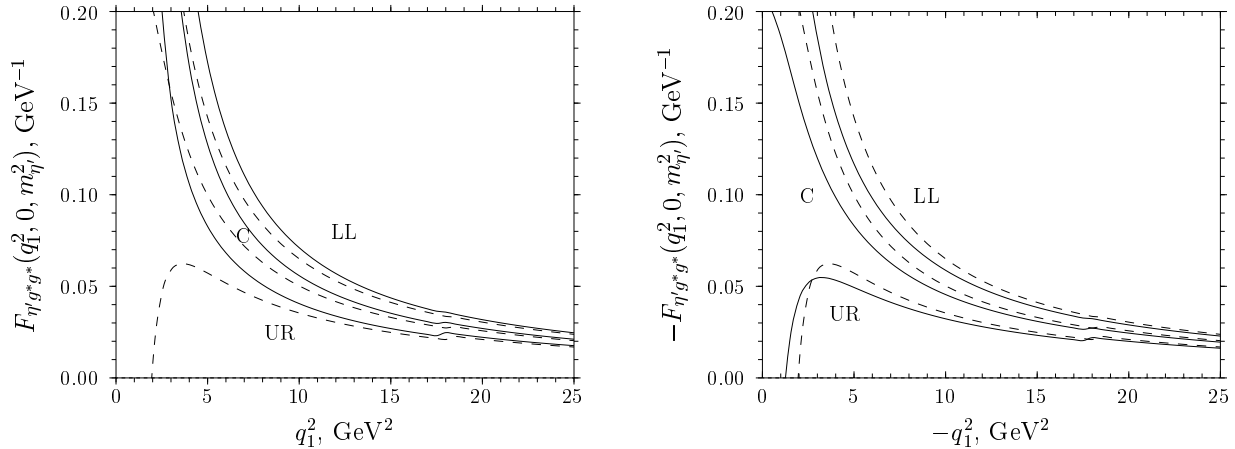


Figure 5: The  $\eta'g^*g$  effective vertex function for the time-like (left frame) and space-like (right frame) gluon virtuality  $q_1^2$  when the second gluon is on the mass shell ( $q_2^2 = 0$ ). The solid and dashed curves are plotted for the vertex function with and without taking into account the  $\eta'$ -meson mass, respectively. The labels C, LL, and UR correspond to the central, lower-left and upper-right points of the combined best fit of the Gegenbauer coefficients  $B_2^{(q)}(\mu_0^2)$  and  $B_2^{(g)}(\mu_0^2)$  presented in Fig. 5 of Ref. [9] and given in Eq. (81).

of the  $\eta'$ -meson mass effect has led to a rather reliable estimate of this vertex function (or the transition form factor) for  $q_1^2 \geq 2 \text{ GeV}^2$  for the time-like region, with a power-like fall-off with  $q_1^2$ , similar to the one seen in the electromagnetic transition form factors of the pseudoscalar mesons [25, 26]. For the space-like gluon virtuality, the vertex function has a power-like fall-off as well, but the current uncertainty in the Gegenbauer coefficients still leaves a rather large dispersion in the vertex function, in particular for the region  $|q_1^2| \lesssim 3 \text{ GeV}^2$ . We expect that more precise data, such as from the decay  $\Upsilon(1S) \rightarrow \eta' X$ , will significantly reduce this parametric uncertainty. In the next section, we show that imposing the anomaly constraint on the vertex function  $F_{\eta'g^*g}(q_1^2, 0, m_{\eta'}^2)$  at  $q_1^2 = 0$  considerably reduces this uncertainty for low values of  $q_1^2$  in the space-like region.

## 5 An Interpolating Formula for the $\eta'g^*g$ Vertex Function for Space-Like Gluon Virtuality

As noted earlier, the QCD anomaly determines the value of the vertex  $F_{\eta'gg}(0, 0, m_{\eta'}^2)$  for on-shell gluons. Denoting this by  $F_{\eta'gg}^A$ , one has the following expression for this quantity [2]:

$$F_{\eta'gg}^A = -4\pi\alpha_s(m_{\eta'}^2) \frac{1}{2\pi^2 f_{\eta'}}. \quad (82)$$

For large off-shellness of the gluons, the form of the vertex function is determined by the perturbative QCD and is presented in Eq. (77). We would like to write down an expression for the vertex function in question which interpolates between the non-perturbative result (82), applicable at  $q_1^2 = q_2^2 = 0$ , and the perturbative QCD result (77), which holds

for large virtualities of the gluons. Such a formula is of considerable phenomenological interest.

Let us concentrate on the case of the  $\eta'g^*g$  effective vertex function with one gluon (the second gluon, for definiteness) being on the mass shell. Comparing Eqs. (67) and (75) with the form (1), it is seen that both the quark-antiquark and the gluonic parts of the  $\eta' - g$  transition form factor have a pole singularity for the time-like virtuality at  $q_1^2 = m_{\eta'}^2$ . However, there is no singularity for the space-like region of the gluon virtuality and the vertex function  $F_{\eta'g^*g}(q_1^2, 0, m_{\eta'}^2)$  is a smooth function of  $q_1^2$  in this region (albeit numerically uncertain due to the imprecise knowledge of the Gegenbauer coefficients). It is also known from our earlier work [2] that the singularity for the time-like region can only be removed by including the transverse momentum effects in the  $\eta'$ -meson wavefunction, using the Sudakov resummation technique. Since we are ignoring the transverse-momentum effects in calculating the vertex function in question in this paper, we shall restrict ourselves to the interpolating function only in the space-like region, for which the transverse-momentum effects are known to be numerically small [2].

To that end, we work with the function  $H(q_1^2, 0, m_{\eta'}^2)$  presented in Eq. (78). It should be noted that the function  $G_2^{(g)}(1, \eta)$  entering in  $H(q_1^2, 0, m_{\eta'}^2)$  is very close to its asymptotic value  $1/6$  already at  $q_1^2 \simeq -1 \text{ GeV}^2$  in the space-like region of the gluon virtuality (see Fig. 4). So, to a very good approximation, the function  $G_2^{(g)}(1, \eta)$  can be replaced by its asymptotic value:

$$H_{\text{as}}(q_1^2) = \frac{4\pi\alpha_s(Q^2)}{m_{\eta'}^2} \sqrt{3}f_{\eta'} \left[ 1 + A_2(Q^2) - \frac{5}{36} B_2(Q^2) \right], \quad (83)$$

with the corresponding vertex function now given by  $F_{\text{as}}(q_1^2) = m_{\eta'}^2 H_{\text{as}}(q_1^2)/(q_1^2 - m_{\eta'}^2)$ . Thus, the dependence of  $H_{\text{as}}(q_1^2)$  on  $q_1^2$  is coming only through  $Q^2 = |q_1^2| + m_{\eta'}^2$ . Defined in this way, the function  $H_{\text{as}}(q_1^2)$  is symmetric under the change  $q_1^2 \rightarrow -q_1^2$ , and has *formally* the following limit for on-shell gluons ( $q_1^2 = 0$ ):

$$H_{\text{as}}(0) = \frac{4\pi\alpha_s(m_{\eta'}^2)}{m_{\eta'}^2} \sqrt{3}f_{\eta'} \left[ 1 + A_2(m_{\eta'}^2) - \frac{5}{36} B_2(m_{\eta'}^2) \right]. \quad (84)$$

Not unexpectedly, there is a substantial mismatch between the correct value of the vertex function for the on-shell gluons  $F_{\eta'gg}^A$ , as determined by the QCD anomaly, and the one obtained from the formal limit of the perturbative expression for the vertex function  $F_{\eta'g^*g}(0, 0, m_{\eta'}^2) = -H_{\text{as}}(0)$ , given in Eq. (84). To see this quantitatively, we study the numerical consistency of the two expressions, which yields the following condition on the Gegenbauer moments  $A_2(m_{\eta'}^2)$  and  $B_2(m_{\eta'}^2)$ :

$$\frac{2\sqrt{3}\pi^2 f_{\eta'}^2}{m_{\eta'}^2} \left[ 1 + A_2(m_{\eta'}^2) - \frac{5}{36} B_2(m_{\eta'}^2) \right] = 1. \quad (85)$$

For the values of the Gegenbauer coefficients given in Eq. (81), this equality is badly violated. For example, for the set of the Gegenbauer moments  $A_2(m_{\eta'}^2) = -0.11$  and  $B_2(m_{\eta'}^2) = 2.87$ , corresponding to the coefficients called LL (yielding the largest value for the l.h.s. in Eq. (85)), the l.h.s. in the above equation is about 0.43. For other allowed

values of the Gegenbauer coefficients, the mismatch is much more pronounced. This implies the presence of large non-perturbative contributions to the moments  $A_2(m_{\eta'}^2)$  and  $B_2(m_{\eta'}^2)$ . However, it is certain that non-perturbative corrections in the vertex function  $F_{\eta'g^*g}(q_1^2, 0, m_{\eta'}^2)$  are to be included over a larger region of  $q_1^2$ .

To model these non-perturbative effects, we propose the following modification of the perturbative result (83) in the region of the small space-like virtualities  $q_1^2$  in terms of the function  $\tilde{H}(q_1^2)$ :

$$\tilde{H}(q_1^2) = H_{\text{as}}(q_1^2) + [H_A - H_{\text{as}}(0)] \exp \left[ C_s \frac{q_1^2}{m_{\eta'}^2} \right], \quad (86)$$

with the corresponding vertex function defined as:  $\tilde{F}(q_1^2) = m_{\eta'}^2 \tilde{H}(q_1^2)/(q_1^2 - m_{\eta'}^2)$ . Here,  $H_A = -F_{\eta'gg}^A$  is defined by the anomaly value for the  $\eta'gg$  vertex in Eq. (82) and  $C_s$  is an arbitrary dimensionless parameter.

This formula gives, by construction, the correct value for the  $\eta'gg$  vertex function with the on-shell gluons (i.e., for  $q_1^2 = 0$ ), reproducing the QCD anomaly, and yields the correct perturbative-QCD behaviour for large values of  $q_1^2$ . Depending on the value of the parameter  $C_s$ , the perturbative result may set in rather fast. For small values of the gluon virtuality, expanding the exponential factor in  $q_1^2/m_{\eta'}^2$  gives power corrections. In the numerical analysis presented below we take  $C_s = 2$ , as it allows a smooth interpolation between the anomaly (at  $q_1^2 = 0$ ) and the perturbative result for  $|q_1^2| > 2 \text{ GeV}^2$ . However, we must admit that this interpolating formula is by no means unique, and has to be checked against experimental data on processes involving the  $\eta'$ -meson, or else compared with the results obtained using non-perturbative techniques, such as the lattice-QCD.

The perturbative vertex function  $-F_{\text{as}}(q_1^2)$  (dashed curves) and the interpolating function  $-\tilde{F}(q_1^2)$  (solid curves) are plotted as functions of  $q_1^2$  in Fig. 6 (left frame). The function  $H_{\text{as}}(q_1^2)$  (dashed curves), defined in Eq. (83), and the corresponding interpolating function  $\tilde{H}(q_1^2)$  (solid curves), introduced in Eq. (86), are shown in the right frame of this figure. The curves are marked as C, LL, and UR, corresponding to the three sets of values for the Gegenbauer coefficients as in Fig. 5. It is obvious that imposing the anomaly condition as a normalization point changes the  $\eta'g^*g$  vertex function in a significant way for low space-like values. For our choice of the interpolating function, this change is marked for  $|q_1^2| \lesssim 1 \text{ GeV}^2$ , increasing the absolute value of the function, and reducing the theoretical dispersion on the vertex function in this region arising due to the imprecise knowledge of the Gegenbauer coefficients in the perturbative expression.

## 6 Conclusions

We have calculated the  $\eta'g^*g^{(*)}$  effective vertex function in the perturbative QCD approach using the light-cone DAs for the  $\eta'$ -meson with the inclusion of the  $\eta'$ -meson mass. It is shown that if one of the gluons is on the mass shell, the pole-like behaviour (1) of the  $\eta'$  - gluon transition form factor emerges in this approach for both the quark-antiquark and the gluonic parts of the form factor, and the corresponding function  $H(q_1^2, 0, m_{\eta'}^2)$  is perturbatively calculated. The Gegenbauer coefficients, required for a quantitative

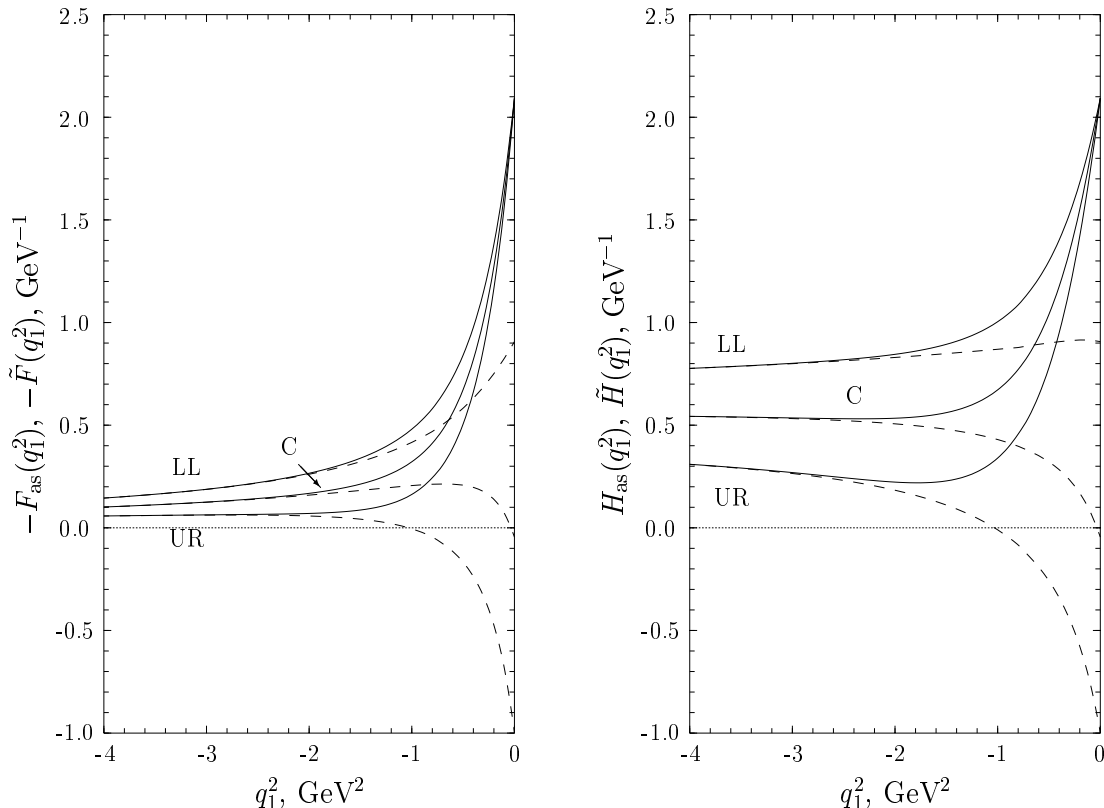


Figure 6: The  $\eta' - g$  transition form factor in the perturbative QCD approach and using the interpolating formula for the space-like region of the gluon virtuality  $q_1^2$ . The left frame shows the functions  $F_{\text{as}}(q_1^2)$  (dashed curves) and  $\tilde{F}(q_1^2)$  (solid curves). The right frame shows the functions  $H_{\text{as}}(q_1^2)$  (dashed curves) and  $\tilde{H}(q_1^2)$  (solid curves). The labels on the curves are the same as in Fig. 5.

analysis of the vertex function, have been taken from the combined analysis of the  $\eta' - \gamma$  transition form factor and the  $\Upsilon(1S) \rightarrow \eta' X$  decay, reported by us earlier in Ref. [9]. The corrections due to the  $\eta'$ -meson mass are analyzed numerically, with the result that they are important for lower values of the gluon virtuality, in particular in the time-like region. An interpolating formula connecting the QCD anomaly value and the perturbative-QCD behaviour of the  $\eta' - g$  transition form factor is presented for the space-like gluon virtuality, taking into account the  $\eta'$ -meson mass, which modifies the vertex function significantly in the region  $|q_1^2| < 1 \text{ GeV}^2$  and reduces the theoretical dispersion in low  $|q_1^2|$  region considerably.

## Acknowledgements

We would like to thank Peter Kroll and Kornelija Passek-Kumericki for helpful correspondence. We also thank Alex Kagan, Christoph Greub, and Sheldon Stone for numerous discussions. The work of A.Ya.P. has been supported by the Schweizerischer National-



fonds.

## References

- [1] T. Muta and M. Z. Yang, Phys. Rev. D **61** (2000) 054007 [arXiv:hep-ph/9909484].
- [2] A. Ali and A. Y. Parkhomenko, Phys. Rev. D **65**, 074020 (2002) [arXiv:hep-ph/0012212].
- [3] P. Kroll and K. Passek-Kumericki, Phys. Rev. D **67**, 054017 (2003) [arXiv:hep-ph/0210045].
- [4] S. S. Agaev and N. G. Stefanis, arXiv:hep-ph/0212318.
- [5] A. L. Kagan and A. A. Petrov, arXiv:hep-ph/9707354.
- [6] D. Atwood and A. Soni, Phys. Lett. B **405**, 150 (1997) [arXiv:hep-ph/9704357].
- [7] A. L. Kagan, AIP Conf. Proc. **618**, 310 (2002) [arXiv:hep-ph/0201313]; Y. Chen and A. L. Kagan, Univ. of Cincinnati preprint (in preparation).
- [8] M. Artuso *et al.* [CLEO Collaboration], Phys. Rev. D **67**, 052003 (2003) [arXiv:hep-ex/0211029].
- [9] A. Ali and A. Y. Parkhomenko, CERN Report CERN-TH/2003-096 [arXiv:hep-ph/0304278] (to appear in Eur. Phys. J. C).
- [10] P. Ball, JHEP **9901**, 010 (1999) [arXiv:hep-ph/9812375].
- [11] V. M. Braun and I. E. Halperin, Z. Phys. C **44**, 157 (1989) [Sov. J. Nucl. Phys. **50**, 511 (1989)]
- [12] V. M. Braun and I. E. Halperin, Z. Phys. C **48**, 239 (1990) [Sov. J. Nucl. Phys. **52**, 126 (1990)]
- [13] M. V. Terentev, Sov. J. Nucl. Phys. **33**, 911 (1981) [Yad. Fiz. **33**, 1692 (1981)].
- [14] M. Beneke and M. Neubert, Nucl. Phys. B **651**, 225 (2003) [arXiv:hep-ph/0210085].
- [15] B. Geyer, M. Lazar and D. Robaschik, Nucl. Phys. B **559**, 339 (1999) [arXiv:hep-th/9901090].
- [16] B. Geyer and M. Lazar, Nucl. Phys. B **581**, 341 (2000) [arXiv:hep-th/0003080].
- [17] A. V. Radyushkin, Phys. Lett. B **385**, 333 (1996) [arXiv:hep-ph/9605431].
- [18] T. Ohrndorf, Nucl. Phys. **B186**, 153 (1981).
- [19] M.A. Shifman and M.I. Vysotsky, Nucl. Phys. **B186**, 475 (1981).
- [20] V.N. Baier and A.G. Grozin, Nucl. Phys. **B192**, 476 (1981).

- [21] M. V. Terentev, JETP Lett. **33**, 67 (1981) [Pisma Zh. Eksp. Teor. Fiz. **33**, 71 (1981)].
- [22] A. V. Belitsky and D. Muller, Nucl. Phys. B **537**, 397 (1999) [arXiv:hep-ph/9804379].
- [23] T. Feldmann, Int. J. Mod. Phys. A **15**, 159 (2000) [arXiv:hep-ph/9907491].
- [24] K. Hagiwara *et al.* [Particle Data Group Collaboration], Phys. Rev. D **66**, 010001 (2002).
- [25] S. J. Brodsky and G. P. Lepage, Phys. Rev. D **24**, 1808 (1981).
- [26] T. Feldmann and P. Kroll, Phys. Rev. D **58**, 057501 (1998) [arXiv:hep-ph/9805294].